Rock and Soil Mechanics

Volume 43 | Issue 10 Article 8

11-25-2022

Statistical and regression analyses of sands stiffness in triaxial tests and application of the results

SHARAFUTDINOV Rafael

Rock and Soil Mechanics 2022 43(10): 2873−2886 ISSN 1000−7598
https: //doi.org/10.16285/j.rsm.2022.00006 rocksoilmech.researchcommons.org/journal

Statistical and regression analyses of sands stiffness in triaxial tests and application of the results

SHARAFUTDINOV Rafael

Gersevanov Research Institute of Bases and Underground Structures (NIIOSP), Research Center of Construction, Moscow, Russia

Abstract: The density and stress state significantly impact on the sand stiffness. Many of hardening soil models used for geotechnical computation are based on Duncan-Chang model and do not consider the influence of density on the soil stiffness. In course of triaxial compression of very dense or loose sands, the shear strains rise induces significant changes in density. In order to evaluate the effects of grain size distribution, density, and stress state on stiffness, the results of 962 isotropic triaxial tests on soil samples from 15 Moscow and Minsk construction sites were processed using statistical and regression analysis. As a result, empirical equations enabling evaluation of the effects of density and stress state on stiffness of sands with different particle size distribution were proposed. Comparative analysis of tests performed on alluvial and continental soils from Europe, India, and the United States sites showed that the sand stiffness is in the same range as sands from Moscow and Minsk sites. Proposed equations can be applied for preliminary estimation of the stiffness parameters for finite element method calculation and also can be used in geotechnical models that allow variability, horizontal and vertical distribution of stiffness to be taken into account. Additionally, the semi-empirical relationship based on the Duncan-Chang model, is proposed. The relationship provides more realistic results for loose and extra dense sands affected by large deformations and/or complex loading paths, when the changes in density influence soil stiffness. Generally, geotechnical engineers may utilize the obtained results to apply them to design of complex soil models.

Keywords: laboratory test; deformation; finite-element modeling; numerical modeling; statistical analysis; stiffness; strain

1 Introduction

Triaxial compression is the most common method for characterizing mechanical properties of soil and rock[1−2]. The International Standards ASTM D2850, ASTM D4767, ASTM D7181, ISO 17892-9, BS 1377, GOST 12248.3 regulating the triaxial test mainly focus on the strength parameters of soil[3]. With respect to compression-type problems, the soil stiffness is usually characterized by the oedometer test. However, triaxial test results are used for computing of different soil models that successfully characterize the soil behavior realistically. Therefore, for the past 30 years, triaxial tests have been used to determine soil stiffness[4].

The soil behavior in terms of triaxial compression can be approximated by a hyperbolic function[5−6] using the following equation (Fig. 1).

$$\sigma_1-\sigma_3=\frac{-\varepsilon_a}{\frac{1}{E_i}-\frac{\varepsilon_a}{(\sigma_1-\sigma_3)_{ult}}} \tag{1}$$

where E_i is the initial tangent modulus; ε_a is the axial strain in the direction of deviatoric stress; and $(\sigma_1-\sigma_3)_{ult}$ is an asymptotic value of stress difference.

Using Eq. (1), Duncan and Chang proposed the following equation to estimate tangent modulus E_t for different strain states[7]:

$$E_t=\frac{\frac{1}{E_i}}{\frac{1}{E_i}+\frac{\varepsilon_a}{(\sigma_1-\sigma_3)_{ult}}} \tag{2}$$

After simplification, E_t can be expressed as

$$E_t=(1-R_fS)^2E_i \tag{3}$$

where $S=\frac{\sigma_1-\sigma_3}{(\sigma_1-\sigma_3)_f}$ is stress level; $R_f=\frac{(\sigma_1-\sigma_3)_f}{(\sigma_1-\sigma_3)_{ult}}$ is the failure ratio that is always less than one and derived from test results, $(\sigma_1-\sigma_3)_f=\frac{2c\cos\varphi+2\sigma_3\sin\varphi}{1-\sin\varphi}$, c is the cohesion of soil, φ is the internal friction angle of soil.

The tangent modulus value for any stress conditions can be expressed by following[8]:

$$E_t=(1-R_fS)^2Kp_a\left(\frac{\sigma_3}{p_a}\right)^n \tag{4}$$

where σ_3 is the minor principal stress; p_a is the atmospheric pressure (100 kPa); K is the modulus number; n describes the rate of variation of E_t with σ_3,

Received: 2022-01-24 Revised:2022-04-24
Author: SHARAFUTDINOV Rafael, male, born in 1987, PhD, Senior Researcher, mainly engaged in research in geotechnical engineering. E-mail: linegeo@mail.ru

and it is the power index associated with the stress level S.

Equation (4) results from a standard triaxial test performed at a constant minimum stress rate. For evaluating plane and volumetric strains, the specimen destruction and its stress state should be considered with respect to three principal stresses.

The Duncan and Chang variable stiffness model has been widely applied to FEM analyses of soil–structure interaction[9]. For example, the PLAXIS hardening soil model utilizes the dependence that considers cohesion pressure $c\cot\varphi$ [10]:

$$E_{50} = E_{50}^{\mathrm{ref}}\left(\frac{c\cot\varphi+\sigma_3}{c\cot\varphi+\sigma_{\mathrm{ref}}}\right)^m \tag{5}$$

where E_{50}^{ref} is the reference secant modulus at the mobilization of 50% of the maximum shear strength, corresponding to a reference confining pressure σ_3 assumed as 0.1 MPa. The E_{50} parameter has been considered due to unambiguity of its definition. Similar general principles using E_{50} stiffness are used in hardening soil models implemented in Midas GTS NX, OPTUM, Z-Soil, etc. software.

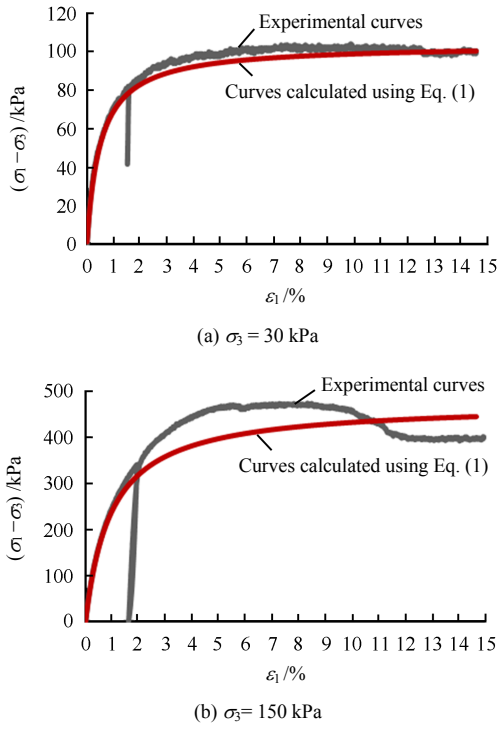

Fig. 1 Results of the test on the medium sand e = 0.52 under a different radial pressure

Nelson et al.[11], Breth, Schuster et al.[12] as well as Nelson et al.[13] proposed more complex variable stiffness models than Duncan and Chang. Corotis et al.[14] proposed a quasi-variable model, in which the strain was considered as a function of stress and strain rates.

The most advantageous feature of the variable stiffness models is its simplicity. However, it precludes the coupling between the deviatoric and volumetric components, which is a significant property of dilatant materials such as cohesionless soil. In addition, none of the proposed variable-stiffness models satisfies the continuity condition[15].

The drawback of the models[7−15] lies in the fact that the accepted relations do not consider the effect of physical properties of soil on shear stiffness. Figure 2 shows the results of triaxial tests on three sand specimens with the same initial void ratio. It is noticeable that during triaxial compression, the void ratio is changing significantly and affects the actual stiffness.

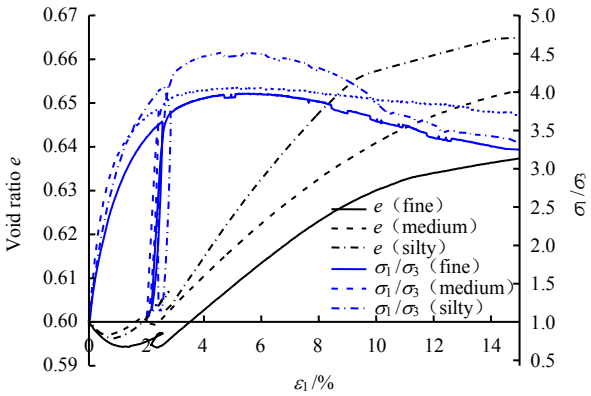

Fig. 2 Results of tests on different sands with the same initial void ratio e_i = 0.6 and confining pressure of 200 kPa

Another essential drawback is that the statistical variability of stiffness is not considered in both the horizontal and vertical directions. For most computational problems, the overall results of calculations show good agreement with observational data. In some cases, for sensitive models, the stiffness distribution significantly affects the settlement, particularly for those with heterogeneous inclusions[16]. In fact, Paice et al.[17] showed that the average settlement could increase by 12% with increasing non-uniformity of the soil under foundation. Furthermore, the bearing capacity could change by 20%–30% with the coefficient of variation of the parameters[18]. This significantly affects the design decisions.

Presently, statistical geotechnical models, which take into account the horizontal or vertical distribution of properties, are becoming increasingly widespread[17−19]. Simulations that consider the soil property distribution

more accurately reflect the basement behavior more realistically[20]. The usage of regression relationships and machine learning methods for developing these calculation methods is very perspective and it is the most powerful tool for studying the influence of factors on soil properties[21−23].

However, existing correlations seldom incorporate the required input parameters for FEM calculation and they are made for specific regions: a few publications[24−25] present the analysis of a limited number of tests and do not encompass particle size distribution or density of most types of sands. In case of variability of physical properties, they do not provide the possibility to evaluate the stiffness with sufficient reliability. The published data do not consider the variability of the soil properties, and therefore, should be used cautiously.

Considering the widespread use of various correlational relationships in engineering practice (at least for preliminary calculations in Russia), a thorough analysis of the experimental data collected for a wide range of sand is conducted.

This paper presents results of the statistical analysis of the stiffness parameters obtained through triaxial compression tests on sand specimens from Moscow and Minsk. A method of evaluation the stiffness E_{50} has been developed considering the grain size distribution, actual stress level, and initial void ratio. The data can be applied for estimation of the sand stiffness without any further testing. Proposed equations can be used in geotechnical models that allow variability, horizontal and vertical distribution of stiffness to be taken into account. Additionally, the semi-empirical relationship based on the Duncan-Chang model, is proposed. The relationship provides more realistic results for loose and extra dense sands affected by large deformations and/or complex loading paths, when the changes in density influence soil stiffness. Generally, geotechnical engineers may utilize the obtained results to apply them to design of complex soil models.

2 General description of investigated soil

Experimental data include results of triaxial compression tests on soil specimens collected at 15 construction sites in Moscow (Russia) and in Minsk (Belarus) (Fig. 3). The sands were classified based on the Russian GOST 25100 classification system, where sand is graded according to the predominant particles' diameter (Table 1). Table 2 shows the physical and mechanical properties of the sand.

The results of 962 isotropic consolidated drained triaxial tests were processed through statistical and regression analysis. Reconstituted soil specimens were prepared from the disturbed soil samples by compacting sand in the air or under water.

During the compaction in the air, dry sand was poured in layers through a funnel on the membrane stretched over a special sample former. Thereafter, the specimen was compacted to a required density either by tamping on the mold or by vibration. The sand compaction under water was performed on the saturated sand. The sand was poured on the membrane filled with water and thereafter compacted to a required density by tapping on the mold or by vibration according to ISO 17892-9-2018[26], ASTM D7181-20[27], and GOST 12248.3-2020[28].

The initial diameter of the test specimen varied from 38 mm to 76 mm and H/D=2. Deviator stress was applied under the stress-controlled or strain-controlled loading mode. Though the loading type is pivotal, according to many studies[29−30], it mainly affects the post-peak parameters which are not considered here.

The test procedure was performed according to GOST 12248.3-2020[28] and conformed to ASTM D7181-20[27] and ISO 17892-9-2018[26].

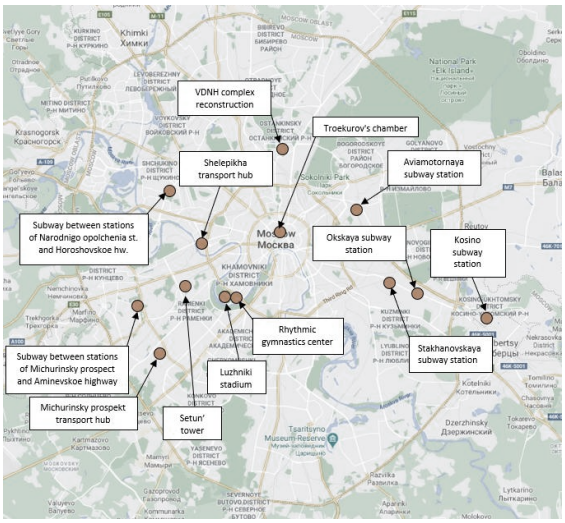

Fig. 3 Layout of the construction site locations

Table 1 Classification of sand based on particle size distribution[28]

Type of sand	Diameter of particles /mm	Particle distribution /%
Gravel sand	> 2	> 25
Coarse sand	> 0.5	> 50
Medium sand	> 0.25	> 50
Fine sand	> 0.10	⩾ 75
Silty sand	> 0.10	< 75

Table 2 Physical and mechanical sand properties of different construction sites

Construction site	Sand age and type	Sample size N	e	c /kPa	φ /(°)	σ_3 /MPa	E_{50} /MPa	E_{ur} /MPa
Okskaya subway station[k]	Q – coarse	3	–	6	34.8	0.05—0.20	22.1—27.9	–
	Q – medium	18	0.35—0.47	4—7	35.7—41.2	0.05—0.30	19.5—60.2	–
	Q – fine	69	0.36—0.71	4—10	29.7—39.6	0.05—0.65	17.1—45.6	–
	Q – silty	33	0.42—0.70	8—11	31.6—38.2	0.05—0.45	17.4—39.1	–
Stakhanovskaya subway station[k]	Q – medium	18	0.58—0.62	1—7	32.1—40.4	0.05—0.55	18.1—44.3	64.5—105.3
	Q – fine	9	0.574	5—7	34.5—37.2	0.10—0.60	28.7—44.0	61.2—88.2
	Q – silty	3	0.606	3—9	34.2—39.2	0.10—0.55	24.7—30.9	62.5—65.6
	J – fine and silty	9	0.44—0.69	6—12	34.9—38.1	0.15—0.75	23.5—51.3	72.5—145.8
Luzhniki stadium[31], [k]	Q – coarse	20	0.50—0.83	1	41.0	0.02—0.06	18.1—39.0	73.5—99.4
	Q – medium	40	0.52—0.87	3—11	34.0—37.0	0.02—0.06	7.9—46.5	60.5—120.0
Subway between stations Michurinsky prospect and Aminevskoe highway[k]	Q – coarse	1	0.48	–	–	0.35	34.1	–
	Q – medium	5	0.50—0.63	1—7	34.0—37.0	0.03—0.75	11.2—41.1	–
	Q – fine	2	0.53	4	35.9	0.27—0.30	32.5—33.0	–
	Q – silty	8	0.54—0.73	3—6	32.2—36.0	0.025—0.32	8.5—25.7	–
	J – fine and silty	5	0.53—0.60	3—5	33.0—34.8	0.47—0.75	29.4—36.5	–
	K – medium	2	0.48	5	35.5	0.27—0.37	35.4—36.0	–
	K – fine and silty	31	0.50—0.73	3—13	31.0—36.0	0.36—0.95	23.5—41.8	–
Subway between stations of Narodnigo opolchenia street and Khoroshovskoe highway[k]	Q – coarse	37	0.44—0.70	0—2	35.8—40.4	0.03—0.28	11.4—52.4	41.7—137.8
	Q – medium	69	0.49—0.77	1—4	30.0—37.0	0.01—0.19	5.0—39.1	19.6—127.6
	Q – fine	47	0.52—0.78	0—7	26.0—35.0	0.02—0.18	8.7—35.9	13.7—107.2
	Q – silty	12	0.54—0.58	6—7	33.0	0.09—0.22	8.4—27.7	27.8—89.4
	J – fine and silty	24	0.48—0.60	4—7	34.0—35.0	0.21—0.57	11.2—33.1	42.0—130.2
	K – fine	6	0.54—0.57	7	36.0	0.12	20.4—29.8	65.0—97.1
	K – silty	6	0.57—0.59	6	35.0	0.12	11.5—18.1	35.8—56.8
NIIOSP experimental site 2018[a, k] [32]	Q – medium	58	0.50—0.70	9—41	29.9—36.3	0.10—1.50	14.9—93.9	52.2—403.0
	Q – fine	27	0.50—0.70	0—22	34.3—40.6	0.10—0.50	17.1—243.0	88.0—234.8
	Q – silty	27	0.50—0.70	9—28	33.8—41.4	0.10—0.50	10.7—113.3	92.4—255.3
Kosino subway station[a,k]	Q – medium	36	0.56—0.64	11—12	35.7—35.8	0.08—0.58	11.4—76.3	74.7—266.0
	Q – fine	36	0.51—0.63	9—22	33.5—36.8	0.08—0.58	5.9—50.9	59.5—248.4
Minsk[s]	Q – medium	38	0.45—0.61	1—82	35.9—39.3	0.25—1.50	25.7—325.0	358.8
	Q – fine	31	0.41—0.63	9—76	35.9—40.6	0.20—1.30	25.0—158.1	239.4～301.4
	Q – silty	4	0.51—0.61	27	39.2	0.20	45.1—47.4	–
VDNH complex reconstruction [k]	Q – coarse	2	–	7	34.9	0.35—0.36	83.9—122.4	390.8—487.7
	Q – medium	5	–	0—7	36.9	0.35—0.52	97.3—140.6	329.7—375.2
Aviamotornaya subway station [k]	Q – medium	45	0.46—0.64	1—6	32.1—39.0	0.01—0.22	6.3—49.6	26.3—184.0
	Q – fine	22	0.53—0.54	6—10	35.8—39.9	0.05—0.13	12.5—29.1	72.4—111.6
	Q – silty	25	0.56—0.57	5—10	30.0—33.9	0.09—0.17	12.5—29.1	53.4—84.1
Shelepikha transport hub [k]	Q – coarse	3	0.50	1	38.0	0.02	3.0—4.0	10.9—15.6
	Q – medium	6	0.53—0.63	1	35.0	0.03	4.2—6.9	12.3—26.4
Setun' tower [k,[25]]	Q – coarse	3	0.49	3	34.0	0.26	22.4—28.5	163.2—175.3
	Q – medium	3	0.63	2	33.0	0.21	36.9—37.7	56.8—88.8
NIIOSP experimental site 2019[a, k] [33]	K – silty	6	0.60	10	35.0	0.37	19.7—39.5	146.2—288.1
	Q – medium	9	0.52	6	36.8	0.03—0.15	9.6—30.6	61.9—119.9
Troekurov's chamber[a]	Q – medium	6	0.60—0.67	1	34.0	0.10	8.6—21.9	–
Michurinsky prospekt transport hub[k]	Q – medium	21	0.64—0.69	2	30.0—32.6	0.12—0.96	7.7—44.2	–
	J – fine	15	0.56—0.59	2—7	27.5—30.0	0.20—0.83	10.5—44.4	–
	K – fine	27	0.54—0.56	1—7	29.0—32.9	0.13—0.73	9.5—35.2	–
Luzhniki rhytmic gymnastic center [k]	Q – coarse	3	0.51—0.53	1	34.0	0.15—0.20	36.1—38.8	–
	Q – medium	8	0.53—0.66	3—6	33.0—35.0	0.10	32.4—43.0	–

Note: a – tests processed by the author; k – strain-controlled loading mode; s – stress-controlled loading mode; Q – Quaternary age; K – Cretaceous age; J – Jurassic age.

The research was carried out on the soil, that comprised Quaternary-age (86.4%), Cretaceous-age (7.6%), and Jurassic-age (6%) sands. The depth of sampling varied from 0.8 m to 58.1 m. The sand

presented here was mainly of quartz or feldspar genesis. The Quaternary sample consisted of alluvial and lacustrine sediments (48%), fluvioglacial and glaciolacustrine sediments (51.7%), as well as moraine sediments (0.3%). The pre-Quaternary sample consisted of the Cretaceous-age (54%) and Jurassic-age (43%) sand.

The following sand parameters were determined from the standard drained triaxial test results: secant modulus determined at 50% strength E_{50}; unloading–reloading modulus determined by the standard (isotropic) drained triaxial test E_{ur} (Fig. 4); Poisson's ratio υ; unloading–reloading Poisson's ratio υ_{ur}; effectives angle of friction and cohesion.

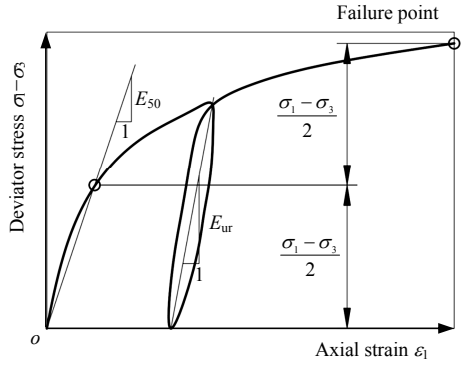

Fig. 4 Definition of stiffness parameters

3 Methods and results of statistical and regression analysis

3.1 Methods

The correlation and regression statistical data analysis technique was employed using MS Excel and IBM SPSS Statistics. The following stiffness parameters were analyzed: stiffness E_{50} and E_{ur}, Poisson's ratios υ and υ_{ur}, and the ratio of unloading–reloading modulus and secant modulus at 50% strength:

$$k_E = \frac{E_{ur}}{E_{50}} \tag{6}$$

At present, these parameters are used as input data for FEM computation for the hardening soil models and are of greatest interest for geotechnical engineers.

It should be noted that the ratio between E_{50}, E_{oed} and E_{ur} is not constant and depends on the type of soil[10]. The k_E parameter was introduced for statistical analysis.

The experimental approach is as follows.

In the first stage, the experimental data were incorporated in a total sample. The strength of relationships was estimated via correlation analysis without considering the particle size distribution. The Pearson's correlation coefficient ρ, significance level (using P-value), and sample correlation ratio η [34-35] were calculated via statistical analysis.

The Pearson's correlation coefficient ρ is widely used in statistical analysis. It evaluates the correlation relationship among the parameters and lies in the ranges from −1 to 1. The closer its value is to 1 (or −1), the stronger is the degree of linear relationship between parameters. If the ρ value is close to zero, it indicates a weak linear strength of relationship

The correlation parameter η is the ratio of a between-group dispersion to the total dispersion. It estimates the strength of the non-linear correlation relation between the parameters and ranges from zero to one. If η is close to zero, the strength of relationship is weak or does not exist; if it is close to one, the relationship is strong. The correlation ratio and the Pearson's correlation coefficient satisfy the condition $\eta \geqslant \rho$.

The correlation analysis revealed the most significant factors and nature of the relationship (linear or non-linear). Relationship in correlation interaction was analyzed at the significance level α =0.05. This corresponds to the GOST 20522 requirements for calculating soil safety factor.

It is well known that stiffness depends on the soil density, stress state, and strength[8, 36−37]. Therefore, the following factors that are considered to affect the soil stiffness were analyzed:

Initial void ratio e_i.

Stress state considered as radial stress σ_3 and relative radial stress[10] that is expressed as:

$$\mathrm{RRS} = \frac{c\cot\varphi + \sigma_3}{c\cot\varphi + \sigma_{3\mathrm{ref}}} \tag{7}$$

Strength properties: the friction angle φ, cohesion c, and cohesion pressure $H = c\cot\varphi$.

Stiffness parameters: E_{50}, E_{ur}, and the Poisson's ratios υ and υ_{ur}.

The RRS parameter includes the reference radial stress and takes into account the dependency of stiffness properties on the soil stress state. Here, the reference pressure σ_{3ref} is considered as 0.1 MPa.

These stiffness parameters were chosen because they were used to characterize sand during engineering surveys at different construction sites (at least in Russia) and in FEM calculations.

In the second stage, the influence of stress state and density was studied in detail, based on the particle size distribution. Due to the variations in the roundness, mineral composition, and admixtures of the sand material, the total sample was provisionally divided into Quaternary and pre-Quaternary groups. Influence of age was not

investigated in detail as all the samples were disturbed, and the soil skeleton as well as the pore voids were not appropriately inspected.

3.2 Analysis of the total sample

The relationships between all parameters are highly non-linear (Table 3). The radial stress σ_3 and RRS considerably affect the sand stiffness E_{50}, E_{ur}. The stiffness–RRS relationship is 10% stronger than the stiffness–σ_3 relationship associated with the strength parameters considered in RRS. However, η between RRS and E_{50} or E_{ur} exceeds ρ by 1.3–1.6 times and η is close to one. It indicates a non-linear relationship. Therefore, it is preferable to use RRS for a more effective description of the relation between stiffness and stress state.

Table 3 Correlation parameters for the total sample

Stiffness parameter		Factor									
		e	σ_3	*H*	*RRS*	φ	*c*	E_{50}	E_{ur}	υ	υ_{ur}
	ρ	−0.18*	0.68*	0.38*	0.62*	0.21*	0.40*	−	−	−	−
E_{50}	η	0.64	0.88	0.77	0.98	0.65	0.70	−	−	−	−
	N	918	962	962	962	962	962	−	−	−	−
	ρ	−0.14*	0.75*	0.42*	0.74*	0.16*	0.49*	0.84*	−	−	−
E_{ur}	η	0.60	0.93	0.82	0.98	0.76	0.66	0.97	−	−	−
	N	520	532	532	532	532	532	515	−	−	−
	ρ	0.05	−0.08*	−0.16*	−0.08	0.01	−0.16*	0.03	0.09	−	−
υ	η	0.44	0.70	0.74	0.82	0.51	0.42	0.86	0.69	−	−
	N	547	587	587	587	587	587	580	322	−	−
	ρ	0.04	−0.25*	−0.02	−0.25*	−0.02	−0.06	−0.28*	−0.24*	−0.03	−
υ_{ur}	η	0.36	0.70	0.58	0.73	0.32	0.45	0.90	0.91	0.80	−
	N	249	249	249	249	249	249	249	248	249	−
	ρ	0.09*	−0.06	0.06	−0.04	−0.02	0.07	−0.31*	0.10*	0.12	0.06
k_E	η	0.55	0.71	0.75	0.87	0.65	0.71	0.89	0.93	0.66	0.92
	N	508	515	515	515	515	515	515	498	322	248

Note: * – correlation relationship at significance level $\alpha = 0.05$.

The initial void ratio has a significant effect on E_{50}, E_{ur}; nonetheless, its effect is less influential than the stress state effect. Non-linear behavior prevails here, and η exceeds ρ by 3.5 times. Similar non-linear influence of density on some types of sands have also been reported[8, 10]. Moreover, the same relationship can be observed during triaxial or oedometer tests. When analyzing the stiffness according to triaxial test results, the essential non-linear influence of the void ratio should be taken into account.

The relationship between stiffness and strength is statistically significant, but it is weak. Poisson's ratios υ and υ_{ur} exhibit a weak relationship, or does not statistically relate with the analyzed factors.

The k_E ratio has a weak relationship with the parameters investigated. However, the relation between E_{ur} and E_{50} is non-linear. With an increase in E_{50} due to an increase in confining pressure and a decrease in the void ratio, E_{ur} increases less intensively (Fig. 5). Nevertheless, for the sake of convenience, a linear relation is appropriate because ρ =0.837 is close to η= 0.967. It is worth mentioning that the determined strength of the relationship is significantly higher than that described previously[25]. This depends on the volume of the data sample and on the wide range of measurements.

In general, the following conclusion can be drawn based on the performed analysis of the total data sample:

Stiffness of sand essentially depends on the radial stress and void ratio and to a lesser extent, on the strength parameters.

Stiffnesses E_{50} and E_{ur} is strongly related to each other.

The Poisson's ratio slightly depends on the physical and mechanical properties of sand.

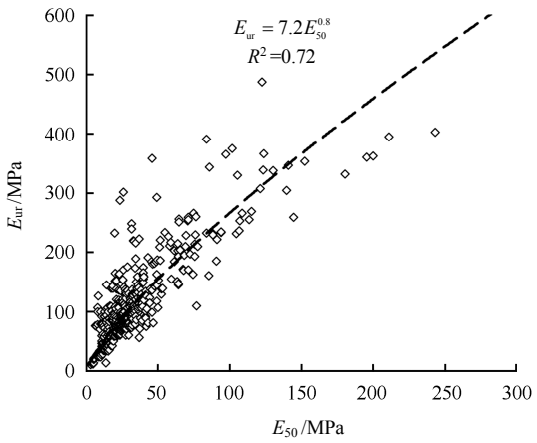

Fig. 5 Relationship between stiffness moduli of the total sample E_{50}–E_{ur}

3.3 Influence of the initial void ratio and radial pressure on E_{50}

Based on empirical data, the diagram showing the dependency of RRS on stiffness E_{50} was drawn (Fig. 6). Lower and upper bonds correspond to the standard deviation for silty and coarse sands, respectively. For particle size analysis, the sample was divided into four provisional zones, depending on the predominance of the different particle sizes: Quaternary sand (A–coarse, B–medium and fine, C–silty) and pre-Quaternary sand (D–fine and silty). With an increasing number of particles of predominant size, the increase in stiffness E_{50} was observed. Stiffness of the pre-Quaternary sands differs from that of Quaternary sand; nevertheless, it partially overlaps with the zone of silty sand.

The smaller values of E_{50} for pre-Quaternary sands are associated with disturbed soil specimens, for which the realistic structure of soil skeleton formed within

the specific period was not considered. Characterization of such soil density via indirect methods (such as CPT) necessitates more extensive investigation. Real stress state and lateral earth pressure coefficient K_0 of such soil may differ from those assumed by the equation[37] corresponding to Quaternary sands. Plate-bearing and pressuremeter field tests provide stiffness E as 35–45 MPa[38–39]. However, the test data showed that stiffness essentially changes for disturbed soils samples. For practical application, it is worth calibrating the triaxial test results against the direct field tests.

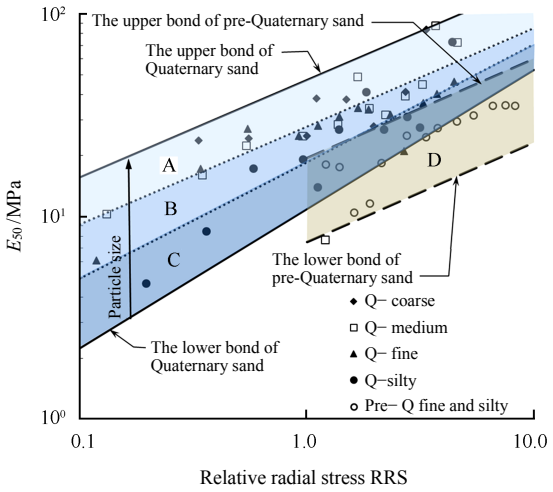

Fig. 6 Influence of the relative radial stress on the stiffness E_{50} of Quaternary (A – coarse; B – medium and fine; C – silty) and pre-Quaternary (D – fine and silty) sand

Figure 6 provides quantitative and qualitative assessment of the effect of RRS on the measured parameters, depending on particle size distribution. With increasing particle size, the intensity of the RRS influence reduces. The degree of relationships for the Quaternary sands is strong and higher than that for the pre-Quaternary sand. The equation obtained may be useful for practical applications:

$$E_{50} = E_{50}^{0.1} \cdot \mathrm{RRS}^{m} \qquad (8)$$

where $E_{50}^{0.1}$ is the reference E_{50} at a radial stress of 0.1 MPa, and m is a power-law coefficient. The values of $E_{50}^{0.1}$ and m depend on grain size distribution for Quaternary sand, their values are respectively equal to: 30 MPa and 0.48 (coarse), 25.4 MPa and 0.5 (medium and fine), and 18.1 MPa and 0.75 (silt) and for pre-Quaternary sand as 13.3 MPa and 0.49. These factors have a high coefficient of determination: $R^2 = 0.59$–0.85.

Equation (8) thoroughly describes the relationship between the stiffness and radial stress without considering sand density. Based on available data, the diagram showing the dependency of initial void ratio on E_{50} was drawn (Fig.7). With decreasing size of particles and increasing void ratio, the value of E_{50} reduces (similar to the Fig. 6), except for coarse sands, where the void ratio slightly affects the stiffness. It is worth mentioning that the presented relations are expressed based on the power law.

Figure 7 shows that the void ratio significantly influences the soil stiffness. Indeed, when e_i changes by 7%–10%, E_{50} may change by 15%–20% on average. With the growing quantity of fine particles, the influence of e_i on E_{50} becomes more significant.

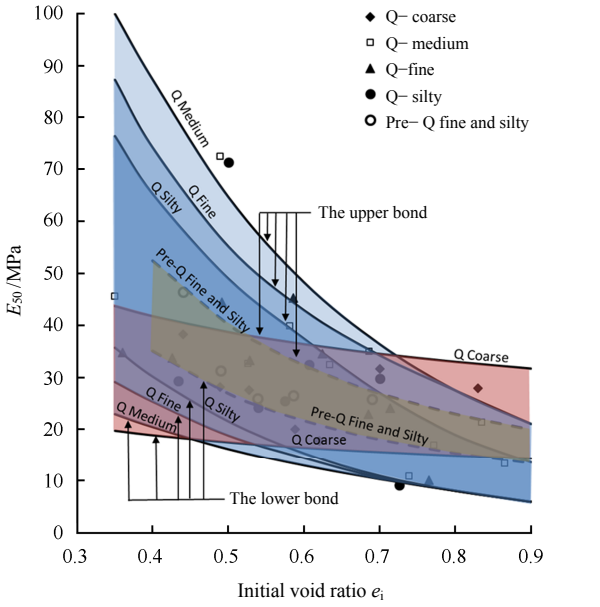

Fig. 7 Influence of the initial void ratio on sand stiffness E_{50}

The relationship incorporating the combined effect of the confining pressure and density on the sand stiffness is shown above. Considering the processed data of large number of triaxial tests performed on sand, the following semi-empirical dependence was proposed:

$$E_{50} = (ae^{b}) \cdot \mathrm{RRS}^{c} \qquad (9)$$

The empirical coefficients a, b, and c can be defined for all types of sand. Accordingly, Table 4 presents a, b, and c values in the Moscow and Minsk regions. Figure 8 shows the results of comparing the design and actual values of E_{50}.

Equation (9) demonstrates variations in stiffness, however, other multifactor models (linear and non-linear)[40] produced less significant results. The values observed and calculated, when compared using Fisher's test, do not reveal any statistically significant difference at the bilateral significance level $\alpha = 0.05$. The existing scatter can be attributed to the large sample size, in-between-laboratory error in stiffness assessment and influence of other factors[41].

Table 4 Empirical coefficients of regression equation for E_{50} for the Moscow and Minsk regions

Empirical coefficients	Quaternary				Pre-Quaternary
	Coarse	Medium	Fine	Silty	Fine and silty
a	31.1	8.1	11.0	12.0	7.76
b	0.051	−1.888	−0.95	−0.691	−1.164
c	0.295	0.731	0.767	0.803	0.432
R^2	0.523	0.668	0.479	0.570	0.557
Standard error	6.3	19.9	21.8	12.4	5.9
N	64	360	237	119	131

In addition, E_{50} defined according to Eq. (9) was compared with other published test results (Table 5). Offshore and barchan sand deposits were not considered since the form of their particles essentially differs from the one that used here. The comparison analysis was made for axisymmetric triaxial test with H/D =2 and for biaxial and triaxial tests with H/D =1.

Table 5 Summary data used for comparison with the results obtained using Eq. (9)

Reference	Sand region	Sand type according Table 1	N	e	σ_3 /MPa	E_{50} /MPa
Desrues et al.[42], II	Hostun (France)	Medium	16	0.659−1.026	0.100−0.800	9.2−105.0
	Manche (France)	Medium	3	1.246−1.270	0.100−0.400	6.2−7.8
Raghunandan et al.[43], I	Kutch district of Gujarat (India)	Coarse	4	0.594−0.685	0.150	22.4−37.7
Wichtmann et al.[36], III	Dorsten (Germany)	Gravel and coarse	31	0.405−0.722	0.100−0.400	8.7−87.7
		Medium	5	0.613−0.754	0.100−0.400	10.0−37.7
		Fine	5	0.650−0.789	0.100−0.400	9.0−57.0
		Silty	11	0.741−0.873	0.100−0.400	8.3−33.5
Varadarajan et al.[44], I	Damuna River (India)	Medium	3	0.600	0.100−0.300	22.0−70.6
Neumann[45], I	Willamette River (USA)	Medium	9	0.607−0.813	0.140−0.410	28.2−317.7
Latini et al.[46], III	Fontainebleau (France)	Fine	9	0.612−0.708	0.050−0.200	17.0−86.3
Ecemis et al.[47], I	–	Fine	2	0.740	0.100−0.200	15.0−30.0
Jansen[48], I	Florida (USA)	Medium	21	0.606−0.874	0.020−0.103	4.5−38.2
Mirnyy et al.[25], I	Moscow (Russia)	Coarse	12	0.550	0.235	31.4
		Fine	42	0.600	0.314	43.9
		Silty	18	0.600	0.170	13.8

Test type: I – triaxial test H/D = 2; II – biaxial test H/D = 3.5; III – triaxial test H/D = 1.

Test results obtained by the other researchers are plotted in Fig. 8. The values of E_{50} in Table 5 fall within the same range as that corresponding to the Moscow and Minsk regions mentioned in Table 2. Results obtained using Eq. (9) agree well with experimental data.

Gravel and coarse sands show a slight scatter in the E_{50} values, evidently associated with compaction of specimens disturbed in the initial part of the deviator loading. This is often observed for soils with loose density and is associated with the quality of sample preparation. In fact, the stiffness of the soil is larger that is confirmed by in-situ tests. Therefore, when interpreting the results of such test, the initial part should be omitted or a short-term loading (to compress the roughness between specimen and top-cap) followed by a slow compression.

The E_{50} values estimated from the results of the plane strain biaxial test are almost similar to those of the axisymmetric triaxial test. This is due to the fact that E_{50} characterizes the plastic strain of the foundation soil. Shear stress in homogeneous soils within the plastic strain limits is similar under both triaxial and biaxial compression (although not identical). However, biaxial compression allows better visualization of the shear process[42].

Furthermore, it has been found that the E_{50} estimated from biaxial test and triaxial test with H/D = 1 slightly differs from triaxial compression with H/D =2. This indirectly indicates that when the specimen collapses, the shear area develops through the area of the smallest resistance. A similar process has been observed for biaxial testing[36]. In the case of H/D = 1, the shear area is formed at an angle of 45° and for homogeneous specimens, this does not significantly affect the measured E_{50}. At the same time, testing with H/D = 1 in some cases provides a higher strength.

In general, Eq. (9) can be used for a generalized evaluation of soil stiffness with sufficient engineering accuracy. The comparison analysis of the foreign data confirms the conclusion that the stiffness of the Moscow and Minsk Quaternary sands insignificantly differs from the sands of the other regions.

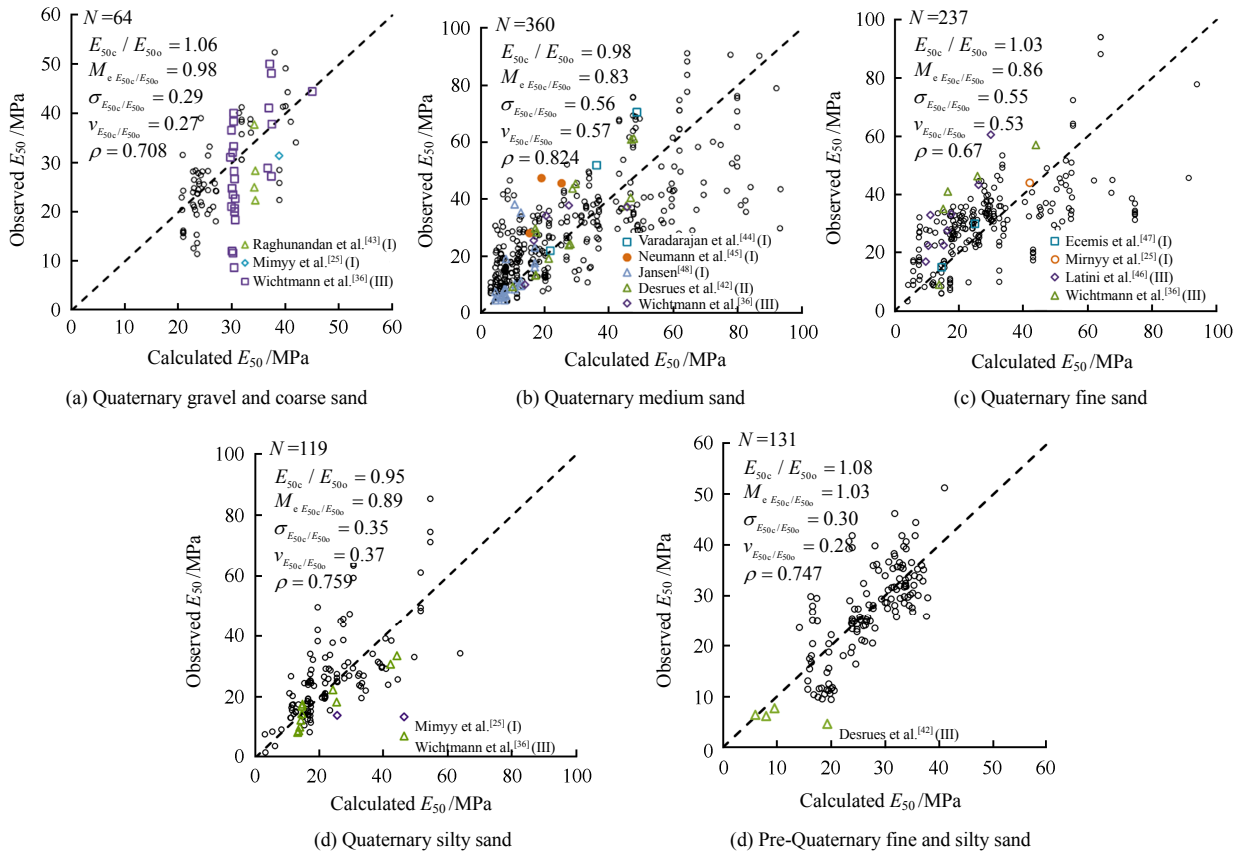

(a) Quaternary gravel and coarse sand (b) Quaternary medium sand (c) Quaternary fine sand

(d) Quaternary silty sand (d) Pre-Quaternary fine and silty sand

Note: I – triaxial test H/D = 2; II – biaxial test H/D = 3.5; III – triaxial test H/D = 1; M_e is the median; the subscripts of c and o mean the calculated and observed values, respectively.

Fig. 8 Comparison results for the observed and calculated E_{50}

3.4 Analysis of the power-law coefficient *m*

The state-of-art non-linear models with isotropic hardening treat the relation between the stiffness and stress state based on Eq. (8). The parameter *m* is used in the models that consider the dependence between stiffness and stress state[7−8,10]. The *m*-parameter can be obtained both on the basis of oedometer test (to identify the compression law) and on the basis of triaxial compression (to identify the dependence of stress state on the shear stiffness).

Table 6 shows the values of *m* estimated from Eq. (8) for various types of sand. It is evident that for Quaternary sand, *m* ranges from 0.46 to 0.85 and appropriately correlates with the experimental data [8,25,49−50]. The value of *m* tends to increase with the decreasing size of particles. However, for medium, fine, and silty sand, *m* changes insignificantly.

In addition, *m* exhibits a downward trend as the soil density increases and doubles when the density of gravel and coarse sand changes from medium to dense. In case of medium sand, it increases by 1.13, and in case of fine and silty sand, it increases by 1.05 and 1.26, respectively. Evidently, the influence of the radial stress decreases with increasing density. Such an effect can be attributed to the internal cohesion that appears when the density increases and affects *RRS* (according to Mohr–Coulomb theory). The described behavior has been revealed based on several processed triaxial tests results, but it contradicts the observation of some researchers. For example, Teo and Wong[50] mentioned that *m* equals 0.45+0.003I_D for sand, that is, *m* increases with the density index I_D. Schanz et al.[4] demonstrated the tendency of *m* to decrease with increasing porosity by performing oedometer tests on Karlsruhe (fine sand) and Hostun and Japanese Toyoura sand (medium sand).

The parameter *m* depends on the testing method. Thus, it can be obtained from either the oedometer or triaxial test results. Under triaxial isotropic compression, *m* ranges from 0.4 to 0.7, and this behavior is not as stable as in the oedometer tests[4].

A small sample size or the fact that the aforementioned researchers did not grade the soils based on particle size distribution could cause this contradiction. In addition, they analyzed the ratio σ_1/σ_a or σ_3/σ_a and did not consider the cohesion pressure $H = c\cot\varphi$. Mirnyy et al.[25] confirmed these studies and demonstrated that *m* increases with *e*.

Table 6 Value of *m* for Quaternary and pre-Quaternary sands

Quaternary				Pre-Quaternary
Gravel and coarse	Medium	Fine	Silty	Fine and silty
$e \leqslant 0.55$			$e \leqslant 0.60$	
0.20	0.75	0.63	0.66	0.47
$0.55 < e \leqslant 0.75$		$0.6 < e \leqslant 0.75$	$0.6 < e \leqslant 0.80$	–
0.41	0.85	0.66	0.83	–

3.5 Analysis of k_E ratio

Table 7 assembles k_E, used in Eq. (6), with respect to the age and particle size of sands. The average value of k_E ranges from 3.46 to 4.64. The k_E ratio does not depend on the age and dispersity of sand. It depends on the strain level at which unloading/reloading is initiated[51].

It has been determined that $k_E \approx 3.8$ can be used for preliminary calculations. Considering this, E_{ur} can be determined from the following expression:

$$E_{ur} \approx 3.8E_{50} \quad (10)$$

The resulting stiffness ratio is extremely close to the data received for some types of sands. Schanz et al.[4] recommended this value as four. However, previous researchers failed to assess the effect of particle size distribution on stiffness. It should be considered that E_{ur} is stress-dependent and should be evaluated based on RRS.

Table 7 Results of statistical analysis of k_E ratio with respect to the age of sands

Sand type	*N*	Average	Median	Standard deviation	Min.	Max.
Pre-Quaternary age						
Fine	18	3.45	3.22	0.78	2.56	4.90
Silty	22	4.13	3.12	2.6	2.57	12.32
Total sample	40	3.78	3.23	1.93	2.56	12.32
Quaternary age						
Coarse	65	3.46	3.25	0.90	2.18	7.30
Fine	117	4.64	3.64	2.43	1.00	15.16
Silty	45	3.48	3.04	1.36	1.88	8.641
Medium	238	3.61	3.19	1.50	1.44	13.55
Total sample	465	3.83	3.28	1.77	1.00	15.16

3.6 Analysis of Poisson's ratio

The outcome of the statistical analysis of Poisson's ratios υ and υ_{ur} is shown in Table 8. The Poisson's ratio υ slightly varies within the range of 0.278 to 0.307 and does not depend on the dispersity of the sand. The unloading–reloading Poison's ratio υ_{ur} varies from 0.164 to 0.194 and does not depend on the dispersity either. In general, the Poison's ratio υ_{ur} can be taken as 0.184 and 0.165 for Quaternary and pre-Quaternary sands, respectively.

Table 8 Results of statistical analysis of Poisson's ratios

Sand type	*N*	Poisson's ratio υ				
		Average	Median	Standard deviation	Min.	Max.
Quaternary age						
Coarse	75	0.307	0.300	0.033	0.25	0.43
Fine	134	0.305	0.300	0.019	0.25	0.38
Silty	63	0.301	0.300	0.019	0.26	0.37
Medium	205	0.306	0.308	0.025	0.23	0.40
Total sample	477	0.305	0.300	0.024	0.23	0.43
Pre-Quaternary age						
Fine	40	0.295	0.292	0.023	0.25	0.39
Silty	46	0.293	0.300	0.032	0.22	0.36
Medium	2	0.278	0.278	0.007	0.27	0.28
Total sample	88	0.294	0.298	0.027	0.22	0.39

Sand type	*N*	Unloading–reloading Poisson's ratio υ_{ur}				
		Average	Median	Standard deviation	Min.	Max.
Quaternary age						
Coarse	41	0.194	0.180	0.047	0.140	0.340
Fine	53	0.174	0.176	0.028	0.110	0.300
Silty	18	0.182	0.172	0.045	0.130	0.340
Medium	88	0.186	0.185	0.039	0.110	0.340
Total sample	200	0.184	0.180	0.039	0.110	0.340
Pre-Quaternary age						
Fine	18	0.164	0.164	0.011	0.150	0.190
Silty	21	0.165	0.178	0.042	0.050	0.200
Total sample	39	0.165	0.170	0.030	0.050	0.200

4 Practical application of the research results

Statistical analysis revealed that the grain size distribution, density of sands, and initial stress state quantitatively affect the stiffness.

Based on statistical analysis, Table 9 shows guideline values of E_{50}. The soil stiffness E_{50} can be selected for various initial void ratios and relative radial stresses. Along with E_{50}, the stiffness E_{ur} can be calculated based on Eq. (10) and *m* can be taken from Table 6. In some cases, the cost of soil testing can be optimized and it allows assigning stiffness characteristics when performing the preliminary calculations. To obtain the final stiffness characteristics for specific soils, it is necessary to confirm the characteristics by direct tests.

The initial stiffness can be described using the hyperbolic Eq. (3)[10]:

$$E_i = \frac{2}{2 - R_f} E_{50} \quad (11)$$

The stiffness in relation to stress level and void ratio can be presented as

$$E_t = \frac{2\left(1 - R_f S\right)^2}{2 - R_f} a e_t^b \mathrm{RRS}^c \quad (12)$$

where e_t is the void ratio at a specific moment of loading $e_t = e_i + \Delta e$, depending on the stress path and

volume strain. Consequently, the volume strain can be considered depending on a stress path, as follows:

Table 9 Guideline values of soil stiffness E_{50} for Quaternary and pre-Quaternary deposits

Sand ages	e	Guideline values of E_{50} (RRS=1−6)					
		1	2	3	4	5	6
				Medium			
Quaternary	0.4	46	76	102	126	148	169
	0.5	30	50	67	83	97	111
	0.6	21	35	47	59	69	79
	0.7	16	26	35	44	52	59
				Fine			
	0.4	26	45	62	77	92	106
	0.5	21	36	50	63	75	86
	0.6	18	31	42	53	63	72
	0.7	15	27	36	46	54	62
				Silty			
	0.4	23	39	55	69	82	95
	0.5	19	34	47	59	71	82
	0.6	17	30	41	52	62	72
	0.7	15	27	37	47	56	65
				Fine and silty			
pre-Quaternary	0.4	23	30	36	41	45	49
	0.5	17	23	28	32	35	38
	0.6	14	19	23	26	28	30
	0.7	12	16	19	21	24	25

Under volume strain,

$$\varepsilon_{vi} - \varepsilon_v = \ln\frac{1+e}{1+e_i} \tag{13}$$

Under shear strain,

$$\mathrm{d}\varepsilon_v^p = \sin\psi\,\mathrm{d}\gamma^p \tag{14}$$

$$e_t = e_i + \sin\psi\,\mathrm{d}\gamma^p\left(1+e_i\right) \tag{15}$$

where ε_{vi} is the initial volume strain; ε_v is the volume strain; ε_v^p is the plasticity volume strain; γ^p is the plasticity shear strain; and ψ is the dilatancy angle.

This approach was tested on silty, fine, and medium sands (Fig. 9) sampled at the NIIOSP experimental site in 2018[32]. Triaxial tests were performed under strain-rate control with initial void ratios e_i = 0.7, 0.6, and 0.5 under confining pressures of 0.1, 0.2, and 0.5 MPa. Specimens were prepared in accordance with the aforementioned technique.

The Duncan–Chang method[7] (Eq.(2)) was compared with Eq. (12) proposed for tangent stiffness. The values were obtained under 2% deformation that did not exceed the expected deformations under most geotechnical impacts[52]. Figure 10 shows the most typical triaxial compression curves and E_t. Table 10 provides comparison results.

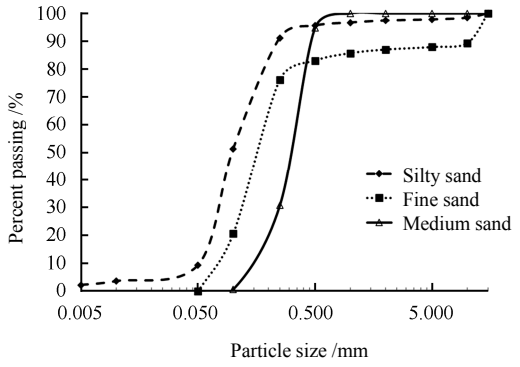

Fig. 9 Cumulative curve of the particle size distribution, plotted for the NIIOSP experimental site 2018[32]

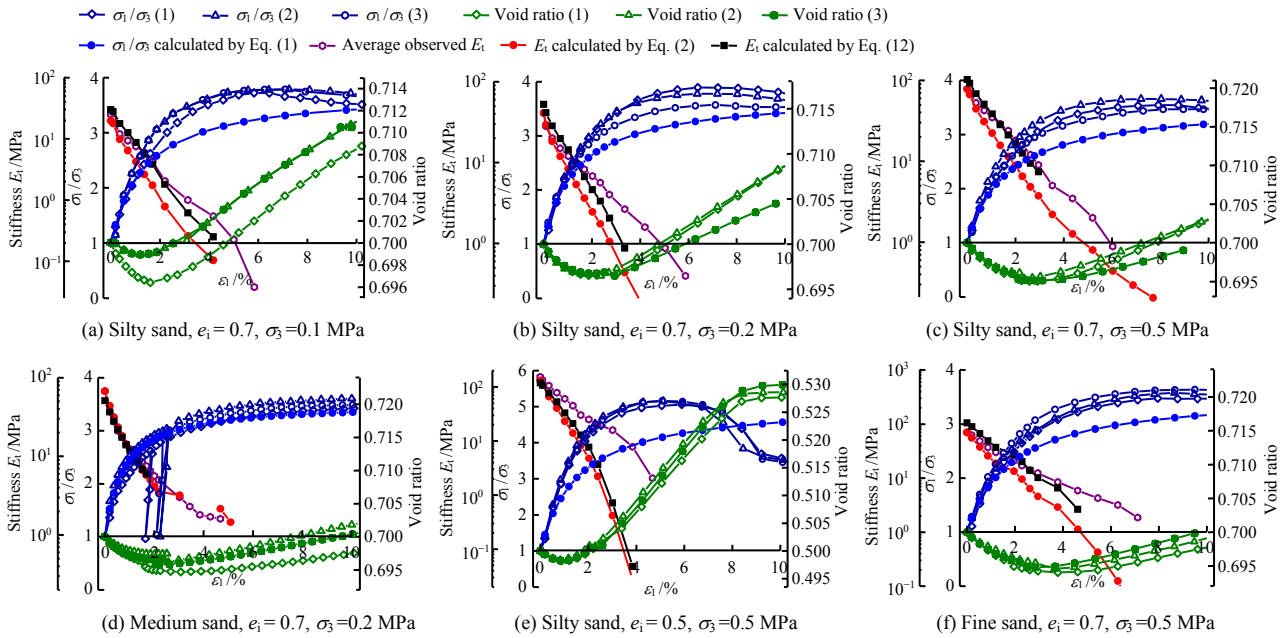

(a) Silty sand, e_i = 0.7, σ_3 =0.1 MPa (b) Silty sand, e_i = 0.7, σ_3 =0.2 MPa (c) Silty sand, e_i = 0.7, σ_3 =0.5 MPa

(d) Medium sand, e_i = 0.7, σ_3 =0.2 MPa (e) Silty sand, e_i = 0.5, σ_3 =0.5 MPa (f) Fine sand, e_i = 0.7, σ_3 =0.5 MPa

Fig. 10 Comparison of average observed and calculated E_t based on Eqs. (12) and (2)[7]

Table 10 Deviation of the observed E_t and calculated E_t using Eqs. (2) and (12) (unit: %)

Type of sand and density	σ_3 =0.1 MPa		σ_3 =0.2 MPa		σ_3 =0.5 MPa	
	Eq. (2)	Eq. (12)	Eq. (2)	Eq. (12)	Eq. (2)	Eq. (12)
Silty sand, e_i = 0.7	−32.0	23.0	−23.0	20.5	38.0	19.0
Silty sand, e_i = 0.6	−2.0	−10.0	−16.0	−10.0	−31.0	−20.0
Silty sand, e_i = 0.5	−9.0	−40.0	−48.0	−50.0	−49.0	−54.0
Fine sand, e_i = 0.7	8.0	−0.4	−14.5	2.5	−19.0	−3.0
Fine sand, e_i = 0.6	−2.0	−10.0	−23.0	2.0	−33.0	−0.5
Fine sand, e_i = 0.5	−34.0	−28.0	−33.0	−21.0	−33.0	−14.0
Medium sand, e_i = 0.7	34.0	34.0	−4.0	−9.0	0.3	−7.0
Medium sand, e_i = 0.6	−2.3	−20.0	−20.0	−25.0	−10.0	11.0
Medium sand, e_i = 0.5	92.0	17.0	−18.0	−6.0	−15.0	−4.4

Calculations performed for both models gave extremely close results. At the same time, Eq. (12) gave less scatter of the E_t values for sands that underwent drastic changes in density during initial loading.

The model corresponding to Eq. (12) describes silty sand with e_i = 0.7 that is 10%–17% better than the model corresponding to Eq. (2). If e_i is 0.6, the average difference between the observed and calculated E_t by Eq. (12) is 9.2%; and the average difference for Eq. (2) is 15.5%. Eq. (12) adequately describes E_t in high-pressure scenarios. In the case of e_i =0.5, Eq. (12) does not provide any advantage: the discrepancy between the actual and calculated E_t is approximately 50% for both the models.

The results for fine and medium sand are the same: with increasing initial void ratio and confining pressure, the calculations using Eq. (12) characterize the soil behavior 20%–30% more accurately, and the values obtained differ slightly from the actual values. The accuracy in calculations performed for dense fine sand with e = 0.5 is also slightly (20%) higher. Variations of E_t appear already during dilatancy.

In general, Eq. (12) provides a more accurate E_t values for loose and dense sands which are characterized by a change in the volume during shear (contraction or dilatancy)[53-54].

The analysis showed that the Duncan–Chang model is suitable for sands undergoing slight changes in density during loading. This refers to specimens with a void ratio of e =0.6. If the specimen suffers drastic changes in density during dilatancy (dense sands e = 0.5 and low confining pressures) or contraction (loose sands or at high confining pressures), the soil stiffness varies significantly. In this case, the proposed empirical dependence matches the stiffness more realistically.

The resulting discrepancies can also be explained by the use of common empirical coefficients a, b, and c. Application of more accurate empirical coefficients for specific sands may produce better results. It is also worth noting that the scatter resulting from the method based on Eq. (12) is lower than the one that based on Eq. (2): generally 1.7 times lower.

Additionally, the tests on loose dense medium sand incorporated several unloading–reloading cycles (Fig. 10(d)), for example, excavation and subsequent load transfer from a building. It was found that with each unloading cycle, additional compaction of sand associated with rearrangement of sand particles occurred due to a change in loading path. Consequently, both the stress state and density of the sands varied, thereby emphasizing the importance of considering the density using Eq. (12). This is particularly important for repeated loading and unloading cycles in multi-stage loading.

If the void ratio insignificantly changes, the derived relationship agrees well with the Duncan–Chang method. Thus, the results of the two approaches were observed to overlap when the volume constantly changes under low-pressure conditions. It can be observed that for loose sands with explicit compaction in the initial stage, the E_t obtained from Eq. (12) within the compaction interval (at ε_1<2 %) is much closer to the actual E_t. Equation (12) is applicable to calculations of significant strain and complex stress paths, when the changes in volume affect the density and stiffness.

Generally, geotechnical engineers may utilize the obtained results, applying them to the simulation of complex soil models.

5 Summary and conclusions

The results of 962 isotropic consolidated drained triaxial tests performed on sand specimens from Moscow (Russia) and Minsk (Belarus) construction sites were processed using statistical and regression analysis. The empirical relationship (Eq. (9)) that considers the mutual influence of the confining pressure and density on sand stiffness was obtained.

Comparison analysis of tests performed on alluvial and continental soils from Europe, India, and the United States sites[25, 36, 42–47] showed that the stiffness E_{50} of the sand is in the same range as soils from Moscow and Minsk sites. Therefore, Eq. (9) is applicable to samples obtained from places outside the Moscow and Minsk regions, with sufficient engineering accuracy.

It has also been found that E_{50} determined from the results of biaxial or triaxial compression with H/D =1 does not differ significantly from E_{50} determined from triaxial compression with H/D =2. This indirectly indicates that when the sample ruptures, the shear area develops

along the area of least resistance. The process is similar to biaxial compression[36]. For H/D =1, the shear area develops at an angle of 45° and should not significantly affect the measured E_{50} of the homogeneous samples. At the same time, testing with H/D =1 in some cases provides higher strength characteristics.

The proposed Eq. (9) can be used in geotechnical models that allow variability, horizontal and vertical distribution of stiffness to be taking into account. This facilitates more accurate modelling of the mechanical behavior in the computational model.

Furthermore, the results of regression analysis can be used for considering change of sand stiffness due to the stress state and density under loading. Based on the Duncan–Chang method[7], a semi-empirical relation (Eq. (12)) is proposed to assess the large deformations and complex loading paths, where the volume and density of the soil change, thereby affecting the stiffness. A comparison of the methods performed at the NIIOSP experimental site[32] showed that the model (Eq. (12)) provides more realistic results consistent with actual E_t values for loose and dense sands typically suffering significant changes in density during shear. This corresponds to the conditions of drastic changes in the sample density during dilatancy (for dense sands, e = 0.5 under low pressure) and contraction (for loose sands or under high pressure). The Duncan–Chang model is well-suited for sands in case of a slight change in density during loading. In case of the need to determine the parameters of Equation (12) for other soil types or for certain sands, regression analysis of drained triaxial test results with different densities and at different confining pressure can be made according to Equation (9).

The m-parameter describes the dependence of the stiffness on the stress state in non-linear hardening soil model[10]. The performed studies revealed the values of the m-parameter depending on the particle size distribution and density (Table 6). However, this parameter depends on the test method. For compression-type problems, it should be determined using oedometer tests. For shear-type problems, triaxial test data should be used.

Numerical values of the ratio of the unloading-reloading stiffness to the secant stiffness at 50% strength k_E were obtained. For sands, the k_E parameter does not depend on the age, particle size distribution and density. The large scatter of data can probably be attributed to the influence of the strain level at which unloading/ reloading was performed[51]. The obtained k_E values are close to those recommended by Schanz et al.[4], that is, four.

An obvious direction for further research is the study of the structure of sand on undisturbed samples. It is also advisable to conduct similar detailed stiffness studies for clay. It is promising to introduce models with the dependence of stiffness on density into the FEM software for large strain problem (for example, PLAXIS, etc.).

Declaration of competing interest

The authors declare that they have no known competing financial interests or personal relationships that could have appeared to influence the work reported in this paper.

Acknowledgements

The author acknowledges the staff of the Laboratory No. 35 of Gersevanov Research Institute of Bases and Underground Structures (NIIOSP) for aid and the materials provided.

References

[1] BISHOP A W, DONALD I B. The experimental study of partly saturated soil in the triaxial apparatus[C]// Proceedings of the 5th International Conference on Soil Mechanics and Foundation Engineering. Paris: Dunod, 1961: 13−21.

[2] MISHRA D A, JANEČEK I. Laboratory triaxial testing - from historical outlooks to technical aspects[J]. Procedia Engineering, 2017, 191: 342−351.

[3] ROSSATO G, SIMONINI P. Stress-strain behaviour of sands in triaxial and direct simple shear tests[J]. Canadian Geotechnical Journal, 1991, 28(2): 276−281.

[4] SCHANZ T, VERMEER P A. On the stiffness of sands[C]//Pre-failure Deformation Behaviour of Geomaterials. London: Thomas Telford, 1998: 383−387.

[5] BOTKIN A I. Investigation of the stress state in cohesiveless and cohesive soils[J]. Bulletin of the Research Institute of Hydraulic Engineering, 1939, 24: 153−172.

[6] KONDNER R L. Hyperbolic stress-strain response: cohesive soils[J]. Journal of the Soil Mechanics and Foundations Division, 1963, 89(1): 115−143.

[7] DUNCAN J M, CHANG C-Y. Nonlinear analysis of stress and strain in soils[J]. Journal of the Soil Mechanics and Foundations Division, 1970, 96(5): 1629−1653.

[8] JANBU N. Soil compressibility as determined by oedometer and triaxial tests[C]//Proceedings of European Conference on Soil Mechanics and Foundation Engineering. Wiesbaden: [s. n.], 1963: 245−251.

[9] WU J T H, TUNG S C Y. Determination of model parameters for the hardening soil model[J].

Transportation Infrastructure Geotechnology, 2020, 7(1): 55−68.

[10] SCHANZ T, VERMEER P, BONNIER P. The hardening soil model: formulation and verification[C]//Proceedings of the Plaxis Symposium. Beyond 2000 in Computational Geotechnics. Rotterdam: Balkema, 1999: 281−290.

[11] NELSON I, BARON M L. Application of variable moduli models to soil behavior[J]. International Journal of Solids and Structures, 1971, 7(4): 399−417.

[12] BRETH H, SCHUSTER E, PISE P. Axial stress-strain characteristics of sand[J]. Journal of the Soil Mechanics and Foundations Division, 1973, 99(8): 617−632.

[13] NELSON I, BALADI G Y. Outrunning ground shock computed with different models[J]. Journal of the Engineering Mechanics Division, 1977, 103(3): 377−393.

[14] COROTIS R B, FARZIN M H, KRIZEK R J. Nonlinear stress-strain formulation for soils[J]. Journal of the Geotechnical Engineering Division, 1974, 100(9): 993−1008.

[15] MIRAYAMA S. Draft of state-of-the-art report on constitutive laws of soils[R]. [S. l.]: ISSMFE Subcommittee on Constitutive Laws of Soils, 1985.

[16] BARVASHOV V A, BOLDYREV G G. Sensitivity of structures and geological data[C]//Proceedings of the 6th ECCOMAS Thematic Conference on Computational Methods in Structural Dynamics and Earthquake Engineering. Rhodes Island, Greece: [s. n.], 2017.

[17] PAICE G M, GRIFFITHS D V, FENTON G A. Finite element modeling of settlements[J]. Journal of Geotechnical Engineering, 1996, 122(9): 777−779.

[18] NOBAHAR A, POPESCU R. Spatial variability of soil properties—effects on foundation design[C]//Proceedings of 53rd Canadian Geotechnical Conference. Montreal: [s. n.], 2000: 1139−1144.

[19] POPESCU R, DEODATIS G, NOBAHAR A. Effects of random heterogeneity of soil properties on bearing capacity[J]. Probabilistic Engineering Mechanics, 2005, 20(4): 324−341.

[20] BOLDYREV G G, BARVASHOV V A, SHEININ V A, et al. Information systems in geotechnical engineering – 3D geotechincs (in Russian)[J]. Geotechnics, 2019, 11(2): 6−27.

[21] GRØNBECH G L, NIELSEN B N. Undrained shear strength determination and correlations on Søvind Marl[C]//Proceedings of the 17th Nordic Geotechnical Meeting. Reykjavík: [s. n.], 2016: 431−440.

[22] THO T X, LONG V T, DU N L. Establishing the correlation of shear strength between consolidated-undrained and consolidated-drained triaxial tests of soft clay[C]//Proceedings of the 10th Slovak Geotechnical Conference. [S. l.]: [s. n.], 2011: 170−174.

[23] ANGELIM R R, CUNHA R P, SALES M M. Determining the elastic deformation modulus from a compacted earth embankment via laboratory and Menard pressuremeter tests[J]. Soils and Rocks, 2016, 39(3): 285−300.

[24] SURARAK C, LIKITLERSUANG S, WANATOWSKI D, et al. Stiffness and strength parameters for hardening soil model of soft and stiff Bangkok clays[J]. Soils and Foundations, 2012, 52(4): 682−697.

[25] MIRNYY A I, BUDOSHKINA K A, SHISHKINA V V. Statistical analysis of hardening soil model mechanical parameters for Moscow region soils (in Russian)[J]. Geotechnics, 2017(4): 58−64.

[26] ISO. ISO 17892-9-2018 Consolidated triaxial compression test on water saturated soils[S]. Geneva: ISO Copyright Office, 2018.

[27] ASTM. D7181-20 Standard test method for consolidated drained triaxial compression test for soils[S]. West Conshohocken, PA: ASTM International, 2020.

[28] GOST R. GOST 12248.3-2020 Soils. Determination of strength and deformation parameters by triaxial compression testing[S]. Moscow: [s. n.], 2020.

[29] CHU J, LEONG W K. Pre-failure strain softening and pre-failure instability of sand: a comparative study[J]. Géotechnique, 2001, 51(4): 311−321.

[30] CHU J, WANATOWSKI D. Effect of loading mode on strain softening and instability behavior of sand in plane-strain tests[J]. Journal of Geotechnical and Geoenvironmental Engineering, 2009, 135(1): 108−120.

[31] SHULYATIEV O A, ISAEV O N, SHARAFUTDINOV R F, et al. Geotechnical aspects of the Moscow Luzhniki Stadium reconstruction[C]//Proceedings of 19th International Conference on Soil Mechanics and Geotechnical Engineering ICSMGE 2017. Seoul: [s. n.], 2017: 2049−2052.

[32] SHULYATIEV O A, ISAEV O N, SHARAFUTDINOV R F, et al. Laboratory studies of a stress state effect on sand deformation characteristics[J]. Bulletin of SRC ‘Stroitelstvo’, 2019, 20: 140−154.

[33] POSPEKHOV V S, SHULYATIEV O A, BAUKOV A U. Corner effect study of the retaining wall design of an experimental excavation in sandy soils (in Russian)[J]. Geotechnics, 2020, XII(1/2020): 16−31.

[34] GMURMAN V E. Guideline for probability theory and mathematical statistic problems solving (in Russian)[M].

Moscow: High School, 2004.

[35] SMOLTCZYK U. Geotechnical engineering handbook[M]. Berlin: Ernst & Sohn, 2002.

[36] WICHTMANN T, KIMMIG I, TRIANTAFYLLIDIS T. On correlations between “dynamic” (small-strain) and “static” (large-strain) stiffness moduli – an experimental investigation on 19 sands and gravels[J]. Soil Dynamics and Earthquake Engineering, 2017, 98(8): 72−83.

[37] MAYNE P W, KULHAWY F H. K_0-OCR relationships in soil[J]. Journal of the Geotechnical Engineering Division, 1982, 108(6): 851−872.

[38] SHULYATIEV O A, ISAEV O N, NAJATOV D V, et al. Forecast of base strains development for a multifunctional residental complex[J]. Geotechnics, 2017(2): 38−49.

[39] SHULYATIEV O A. Soils and foundations of high-rise buildings (in Russian)[M]. Moscow: ASV, 2018.

[40] SHEIN E V. Regression analysis in soil science (in Russian)[M]. Vladimir: [s. n.], 2016.

[41] DMITRIEV V V. Optimization of laboratory geotechnical research[M]. Moscow: Nedra, 1989.

[42] DESRUES J, HAMMAD W. Shear banding dependency on mean stress level in sand[C]//Proceedings of the 2nd International Workshop on Numerical Methods for Localization and Bifurcation of Granular Bodies. Gdansk-Sobieszewo: [s. n.], 1989: 57−67.

[43] RAGHUNANDAN M E, JUNEJA A, BENSON HSIUNG B C. Preparation of reconstituted sand samples in the laboratory[J]. International Journal of Geotechnical Engineering, 2012, 6(1): 125−131.

[44] VARADARAJAN A, MISHRA S S, WADHWA G L. Effects of stress-path on the stress-strain-volume change relationships of a river sand[C]//Proceedings of 3rd Australia-New Zealand Conference on Geomechanics. Wellington: [s. n.], 1980.

[45] NEUMANN D. Hyperbolic soil parameters for granular soils derived from pressuremeter tests for finite element programs[D]. Portland: Portland State University, 1987.

[46] LATINI C, ZANIA V. Triaxial tests in Fontainebleau sand[R]. Kongens Lyngby: Technical University of Denmark, 2016.

[47] ECEMIS N, DEMIRCI H E, KARAMAN M. Influence of consolidation properties on the cyclic re-liquefaction potential of sands[J]. Bulletin of Earthquake Engineering, 2015, 13(6): 1655−1673.

[48] JANSEN J W. Correlating strength and stiffness data of the PENCEL pressuremeter and triaxial compression tests in Florida sands[D]. Melbourne: College of Engineering at Florida Institute of Technology, 2015.

[49] VON SOOS P. Properties of soil and rock (in German)[M]. Berlin: Ernst & Sohn, 1990.

[50] TEO P L, WONG K S. Application of the hardening soil model in deep excavation analysis[J]. The IES Journal Part A: Civil & Structural Engineering, 2012, 5(3): 152−165.

[51] BERSHOV A V, MIRNY, A Y, USOV A N. Determination of the unloading modulus of deformation in dispersive soils and its accounting in designing[J]. Soil Mechanics and Foundation Engineering, 2020, 57(1): 1−7.

[52] ATKINSON J H, SALLFORS G. Experimental determination of soil properties[C]//Proceeding of the 10th European Conference on Soil Mechanics and Founation Engineering (ECSMFE). Florence: [s. n.], 1991: 915−956.

[53] ROWE P W. The stress-dilatancy relation for static equilibrium of an assembly of particles in contact[J]. Proceedings of the Royal Society of London. Series A. Mathematical and Physical Sciences, 1962, 269: 500−527.

[54] SHARAFUTDINOV R F, ISAEV O N, MOROZOV V S. Experimental studies of cohesionless subsoil dilatancy under conditions of triaxial compression[J]. Soil Mechanics and Foundation Engineering, 2021, 57(6): 465−472.